NUMERICAL CALCULATION OF MOTION AND LASER RADIATION HEATING OF PLASMA FORMED DURING ABSORPTION BURST IN VAPORS OF A SOLID BODY

G. G. Vilenskaya and I. V. Nemchinov

We examine the plane (one-dimensional) problem and also the problem with cylindrical or spherical symmetry of the motion and heating by laser radiation of the plasma formed during the absorption "burst" in the vapors of a solid body. The physical basis and mathematical formulation of the problem are given. A numerical method for solving the problem is proposed and results are illustrated by numerical calculation of a specific version in the plane case. Graphs are presented which illustrate the motion-development pattern. Estimates are made of the basic parameters in the vapor layer at various stages: burst criterion, estimate of pressure decrease at the moment of screening initiation, development of the warmup process, and amplitude of the shock wave propagating from the heating zone. The parameters of the detonation wave propagating from the heating zone are evaluated and a comparison is made with the self-similar problem on the self-consistent rarefaction and heating wave. Computational results are presented which show the influence of two-dimensionality on the screening development time.

Under the action of powerful laser radiation flux incident on the surface of a nontransparent solid body, the thin surface layer of its matter is rapidly heated and vaporized. The vapors usually absorb the optical band radiation quite weakly. Therefore, the radiation penetrates through the vaporizing and expanding vapor layers into the deeper layers of the matter, causing their heating, vaporization, and so on – a vaporization wave develops [1-6]. As the vaporization wave advances and the mass of the vaporized matter and the thickness of the vapor layer increase, the pressure gradient decreases. Therefore, cooling as a result of expansion decreases, becoming comparable at some "critical" moment of time with the heating due to absorption of radiation by the weakly ionized vapors. Local temperature rise begins and the temperature rise rate increases rapidly. This is associated with the nonlinear temperature dependence of the absorption coefficient at low temperatures (on the order of the phase change temperature) and the low degrees of ionization, which increase in the presence of thermodynamic equilibrium in accordance with the Boltzmann exponential law. Consequently, we have the process of rapid increase of the temperature, the degree of ionization, and, therefore, the absorption coefficient. An absorption "burst" occurs, and because of the luminosity increase it is a burst in the direct sense of the word. The ionized layer of matter absorbs all the incident radiation and vaporization ceases. The narrow energy release zone becomes a region of high pressure, a compression wave develops, and the shock wave propagates opposite the radiation flux. The degree of ionization of the vapors behind the front of this shock wave and the corresponding optical radiation absorption coefficient are quite large, and absorption of the radiation takes place only in the narrow zone near the shock wave front. The shock wave intensifies and changes into a detonation wave [7, 8]. After the detonation wave reaches the boundary with the vacuum, the layers of low-mass matter adjacent to this boundary are heated up rapidly and spread out, their optical thickness decreases, the radiation begins to penetrate into the deeper layers of the matter, i.e., a self-consistent rarefaction and heating wave propagates [9-11], traveling toward the surface of the solid body. Ahead of it the shock wave propagates, reflecting from the surface of the solid body. Pressure oscillations develop on this surface. After the rarefaction and heating wave approaches the surface of the solid body, the vaporization renews. The hot vapor layer is effectively forced back from the surface of the solid body by the colder vapors, which have

Moscow. Translated from Zhurnal Prikladnoi Mekhaniki i Tekhnicheskoi Fiziki, Vol. 10, No. 6, pp. 3-19, November-December, 1969. Original article submitted March 20, 1969.

a temperature close to the phase-change temperature. The critical conditions may be reached again in this layer and then another burst occurs. The vaporization process thus has a pulsating nature. This process can be considered continuous only for a screening initiation time which is much less than the characteristic exposure time.

Notation. u = velocity; ρ = density; v = specific volume ($v = 1/\rho$); p = pressure; e = internal energy; T = temperature; T_v = equilibrium temperature of vapor and condensate; Q = heat of vaporization; x = vapor fraction in mixture of vapor and condensate; h = enthalpy; H = effective "combustion" enthalpy; q = radiation flux density; $F = qr^{\nu-1}$ = total radiation flux; r = Eulerian coordinate; $\nu = 1, 2, 3$ in the plane, cylindrical, and spherical cases respectively; m = Lagrangian mass coordinate; t = time; c = speed of sound; k = differential adiabatic exponent; γ = effective (integral) adiabatic exponent; $\varkappa$ = mass absorption coefficient; R = universal gas constant; C_p and C_v = specific heats; and μ = molecular weight of the matter.

A "plus" index relates to the reflected radiation flux, a "minus" index relates to the incident radiation flux; s relates to the condensed phase; g relates to the gaseous phase; W relates to the parameters behind the vaporization wave; 0 relates to the parameters ahead of the vaporization wave (in the unvaporized matter); and an asterisk relates to the moment of burst.

1. PROBLEM FORMULATION

Basic Assumptions. In the region in question, in which we calculate the motion and the heating, the medium is in the thermodynamic equilibrium state (this applies to ionization equilibrium – and herein lies the difference between the considered phenomena of weakly ionized vapor heating and nonequilibrium breakdown in cold gases [7, 8] – and also to the equilibrium between the condensed and vaporous phases). In the latter case we also assume the existence of mechanical and thermal equilibrium between the phases.

We neglect the heat transfer processes: conventional and electronic thermal conduction, thermoelectronic emission from the surface of the condensed phase, diffusion of electrons, and also reradiation by the heated plasma.

We assume that reflection takes place at the surface of the solid body or at some effective reflecting surface in the equilibrium mixture of vapor and droplets, where the condensate concentration is sufficiently high. In the remaining region there is no reflection or scattering. The reflection takes place specularly with the effective reflectivity k_r determined from experiments prior to beginning of surface screening by the vapors, or equal to its value under conventional conditions (its tabulated value) if such experimental data are not available. We also examine the opposite limiting case – absence of condensation behind the vaporization wave.

The system of equations describing the motion and heating of the vapors has the following form:

equation of motion

$$\frac{\partial u}{\partial t} + r^{\nu-1}\frac{\partial p}{\partial m} = 0 \tag{1.1}$$

equation of continuity

$$\frac{\partial v}{\partial t} - \frac{\partial (u r^{\nu-1})}{\partial m} = 0 \tag{1.2}$$

energy equation

$$\frac{\partial (e + u^2/2)}{\partial t} + \frac{\partial (p u r^{\nu-1})}{\partial m} + \frac{\partial F}{\partial m} = 0 \tag{1.3}$$

transport equations for incident and reflected radiation

$$\frac{\partial F^+}{\partial m} = -\varkappa F^+ r^{-\nu+1}, \quad \frac{\partial F^-}{\partial m} = \varkappa F^- r^{-\nu+1}, \quad F = F^+ + F^- \tag{1.4}$$

equation of state and absorption coefficient dependence on the thermodynamic parameters:

for $T > T_V(p)$ (or $e > e_V(p)$)

$$p = e\rho(\gamma - 1),\ \gamma = \gamma(e, \rho),\ \varkappa = \varkappa(e, \rho) \tag{1.5}$$

for $e < e_V(p)$ (in the two-phase region)

$$T = T_v(p),\ e = e_g x + e_s(1 - x)\ v = v_g x + v_s(1 - x),\ p = p_g = e_g\rho_g(\gamma - 1) \tag{1.6}$$
$$\varkappa_g = \varkappa_g(e_g),\ \varkappa = \varkappa_g x + \varkappa_s(1 - x)$$

The functions $\gamma(e, \rho)$, $\varkappa(e, \rho)$, $e_g(\rho)$, $\gamma_g(e_g)$, $e_s(e_g)$, $\varkappa_g(e_g)$ are assumed given.

In the two-phase region there is a single-valued connection between the pressure and temperature; therefore the vapor internal energy e_g depends only on the temperature, in spite of the possible processes of atom association into molecules and their dissociation, and also weak ionization.

The pressures are assumed quite low in comparison with the bulk modulus of the condensed phase and the critical pressure in the gaseous phase; therefore $v_S = v_0$, where v_0 is the specific volume corresponding to the normal density of the solid body.

The tables of $\gamma(e, \rho)$ and $\varkappa(e, \rho)$ for the vapor outside the two-phase region, and also $\gamma(e)$ and $\varkappa(e)$ within this region, are calculated with account for the ionization processes, both single and multiple ionization and sometimes even complete ionization, since very high temperatures can be reached when using laser radiation to heat vapors.

In the calculations of the equation of state no account was taken for nonideal gas effects, which may be significant in certain cases because of the high vapor densities.

In the first rough approximation at low temperatures we can set

$$e_g = (C_v)_g T,\ e_s = (C_v)_s T = 3RT/\mu,\ \gamma = 5/3 \tag{1.7}$$

and represent the relation $T_V(p)$ in the form

$$\lg(p) = a(T) - \mu Q/RT_v = a(T) - b/T_v \tag{1.8}$$

In the high-pressure region the relation $T_V(p)$ is often unknown; then the calculation using (1.8) is made using the last (reference) theoretical or experimental point $T = T_0$ in the region of comparatively low pressures, and then either by direct extrapolation of $a(T)$ or simply by setting $a = a(T_0)$.

The absorption coefficient of the vapors is calculated with account for variation of the degree of ionization. In the concrete calculations of the absorption coefficient we took into account free-free electron transitions in the field of neutral atoms and ions, free-free absorption from the highly excited states, and in certain cases molecular absorption (Swan bands for carbon), and also absorption as a result of electron detachment from negative ions.

Vaporization Wave. If the zone in which the phase change takes place is sufficiently narrow in comparison with the characteristic dimensions of the problem and can be considered effectively a discontinuity then the propagation of this zone can be described on the basis of the conservation laws across this discontinuity. Such a wave will be a deflagration type wave [12], since it travels quite slowly with respect to the matter ahead of it and sonic disturbances overtake it, creating in the unvaporized matter a pressure, which will be the unknown parameter.

The conservation laws and the condition of phase equilibrium of the vapor and condensed matter alone, and also the Jouguet condition behind the wave or the condition of compatibility of the wave motion with the flow behind it for subsonic vapor efflux, will not be sufficient for determining its velocity, even for a known magnitude of the radiation flux density q_W supplied to the vaporization wave. Some other physical condition must be added. Here we shall use the condition of a given degree of vaporization completion, i.e. a given value of x_W, which has the following meaning.

In contrast with the ideas of [1-4], in the present study, as in [5, 6], we assume that phase equilibrium is established for sufficiently long duration of the process at some section which is not far from the vaporizing surface, regardless of whether the vaporization is surface or volumetric. If we assume that the matter behind the wave is completely vaporized and the vapors are transparent, then they begin to expand adiabatically, their temperature decreases, and condensate must appear in them. The condensate particles begin to absorb the radiation markedly. Such absorption by the condensate plays a fundamental role in determining the vaporization wave propagation velocity.

Specifically, according to [13], for carbon particles the mass absorption coefficient $\varkappa_S = 0.3 \cdot 10^5$ cm^2/g, while even for energy input $E = 2$ J/cm^2 and heat of vaporization $Q = 40$ kJ/g, the vaporized mass m_W exceeds $5 \cdot 10^{-5}$ g/cm^2. Consequently $\varkappa_S m_W \gg 1$ and significant condensation is not possible, since the energy release owing to radiation absorption by the condensate hinders further condensation.

Neglecting radiation absorption by the vapor itself (i.e., assuming that $\varkappa = \varkappa_S (1-x)$, where x is the vapor mass fraction), we find that the transparency condition for the vapor-condensate mixture leads to the condition $\varkappa_S m_W (1-x) \lesssim 1$. For $\varkappa_S m_W \gg 1$ we obtain $(1-x) \ll 1$, i.e., vaporization of the matter is practically complete.

Thus, we can assume that behind the vaporization wave the value of x_W is given, and x_W is either that value of x for which the equilibrium can be considered already established, if this establishment took place for $x \ll 1$, or that value of x for which the width of the vaporization wave's leading edge is quite small in comparison with the characteristic dimension of the problem (so that the calculation is not made in the zone of large parameter gradients). Usually $(1-x_W) \ll 1$; therefore the exact value of x_W is not significant and for many practical applications we can take $x_W = 1$. In those cases in which condensation does not take place behind the vaporization wave, a more detailed analysis of the structure of the vaporization wave is required [3, 4].

Within the framework of the system being considered the calculation can be made either in the limiting case of no condensation, i.e., for surface vaporization, as assumed in [1-4], or for sufficiently short exposure times, when condensate cannot form [4]. In this case Eqs. (1.6) are not used and absorption by the condensate is not taken into account. The additional condition behind the vaporization wave can be taken, for example, in the form of the condition that the transition be isothermal because of strong thermal conductivity [3] or from examination of the wave structure on the molecular-kinetic level [4].

Boundary Conditions. The following boundary condition was taken at the boundary between the vapors and vacuum (for $m = 0$):

$$p = 0, \quad F^- = F_0(t) < 0 \tag{1.9}$$

The following boundary conditions were taken on the vaporization wave (for $m = m_W$), travelling with the velocity $D_W = dm_W/dt$:

a) if the boundary is stationary ($D_W = 0$)

$$u_w = 0 \tag{1.10}$$

b) if the vaporization wave moves ($D_W \neq 0$)

$$x = x_w, \quad F_w^+ = -k_r F_w^-, \text{ or } \quad F_w = F_w^- (1 - k_r)$$

the energy balance condition

$$D_w = \frac{F_w}{h_w + u_w^2/2 + Q} = \frac{F_w}{H} \tag{1.11}$$

continuity

$$u_w = -\frac{D_w}{\rho_w r_w^{\nu-1}} = -\frac{D_w h_w (\gamma_w - 1)}{p_w \gamma_w r_w^{\nu-1}} \tag{1.12}$$

Here the density ρ_W was expressed in terms of h_W and p_W, using (1.5).

The velocity u_W is extrapolated to the front (compatibility of the motion of the vaporization wave with the flow behind it) if it is found that $u_W < c_W$ or the additional Jouguet condition $u_W = c_W$ is assumed. The pressure p_0 at the surface of the solid body is calculated from the momentum equation

$$p_0 = p_w - D_w u_w r_w^{-(\nu-1)} \tag{1.13}$$

Upon satisfaction of the Jouguet condition

$$p_0 = p_w (k_w + 1) \tag{1.14}$$

Initial Conditions. For $t = t_0$ some distribution of the function $u(t_0, m)$, $v(t_0, m)$, $p(t_0, m)$, $r(t_0, m)$ is given for $m_W^\circ \leq m \leq 0$.

2. NUMERICAL CALCULATION METHOD

System of Difference Equations. The difference scheme for (1.1)-(1.4) will be presented for simplicity for the example of the planar case ($\nu=1$). This difference scheme has the form

$$u_i^{n+1} = u_i^n - \xi_i [(p')_{i+1}^n - (p')_{i-1}^n] \tag{2.1}$$

$$v_i^{n+1} = v_i^n - \xi_i [u_{i+1}^{n+1} - u_{i-1}^{n+1}] \tag{2.2}$$

$$E_i^{n+1} = E_i^n - \xi_i [(p')_{i+1}^n u_{i+1}^{n+1} - (p')_{i-1}^n u_{i-1}^{n+1}] - (\partial q / \partial m)_i^n \Delta t \tag{2.3}$$

Here n and n+1 are the numbers of the time steps, and i and i+1 are the numbers of the space steps. The following notations are also introduced

$$E_i^n = e_i^n + (u_i^n)^2/2, \qquad E_i^{n+1} = e_i^{n+1} + (u_i^{n+1})^2/2$$
$$(p')_i^n = p_i^n + f_i^{n+1/2}, \qquad \xi_i = \Delta t / (m_{i+1} - m_{i-1})$$

Since discontinuous solutions, shock waves, may arise in this problem, we introduce into the system of finite difference equations [14] the Neumann viscosity f for the smearing of these shock waves as follows. Let all the parameters be known on the nth time layer. On the (n+1)-th time layer we calculate the velocity u_i^{n+1} in the first approximation, using (2.1) for $f_i^{n+1/2} = 0$. Then we calculate the Neumann viscosity using the relation

$$f_i^{n+1/2} = \varepsilon_1 \Delta m_i^2 (\varepsilon^+ \Delta u_{i+1} + \varepsilon^- \Delta u_{i-1})^2 / 2v_i^n \tag{2.4}$$

Here

$$\varepsilon^+ = 1, \quad \text{if} \quad \Delta u_{i+1} = u_{i+1}^{n+1} - u_i^{n+1} < 0$$
$$\varepsilon^+ = 0, \quad \text{if} \quad \Delta u_{i+1} \geqslant 0$$
$$\varepsilon^- = 1, \quad \text{if} \quad \Delta u_{i-1} = u_i^{n+1} - u_{i-1}^{n+1} < 0$$
$$\varepsilon^- = 0, \quad \text{if} \quad \Delta u_{i-1} \geqslant 0$$

The constant ε_1 is chosen so that the shock wave smears over several computational points. Then the velocity is recalculated using (2.1) and the calculation is made using (2.2) and (2.3).

Analyzing the stability of the selected difference scheme without viscosity [14], we obtain for the infinite problem the limitation on the time step in the form of the Courant condition $\Delta t \leq \Delta m/\rho c$, where c (speed of sound) is calculated by differentiating the equation of state (1.5) or (1.6). Stability analysis of the problem with account for viscosity yields the additional limitation on the time step

$$\Delta t \leqslant \Delta m v / 2\varepsilon_1 |\Delta u|$$

Calculation of Vaporization Wave. Let

$$\varphi_w = \exp\left(-\int_{m_w}^{0} \varkappa(T, \rho)\, dm\right) \tag{2.5}$$

If $\varphi_w > \varepsilon_w$, where ε_w is a given constant, and $q_0(t) = 0$, then the motional wave and the parameters on the vaporization wave are calculated as follows:

$$m_w^{n+1} = m_w^n + D_w^n \Delta t, \qquad u_w^{n+1} = u^{n+1} + u_w^n - u^n, \quad u = u_{w+2} + \frac{m_w - m_{w+2}}{m_{w+1} - m_{w+2}} (u_{w+1} - u_{w+2}) \tag{2.6}$$

(w+1 is the index of the computational point closest to the vaporization wave.)

The iterations continue, which we illustrate by a particular example: let $\gamma = k = \text{const}$, $C_p = \text{const}$, and $T_v(p)$ is described by (1.7) for $a = a_0 = \text{const}$.

$$D_w^{j+1} = \frac{(1-k_r)\varphi_w q_0(t)}{h_w^j + [(u_w^{n+1})^2/2] + Q}, \qquad p_w^{j+1} = \frac{D_w^{j+1} h_w^j (\gamma - 1)}{u_w^{n+1} \gamma}, \qquad T_w^{j+1} = b/[a - \lg(p_w^{j+1})], \quad h_w^{j+1} = C_p T_w^{j+1} \tag{2.7}$$

Here j is the iteration number. After the convergence condition is reached, when $|(h_w^{j+1} - h_w^j)/h_w^j| \leqslant \varepsilon_h$, the following quantities are taken:

$$\rho_w^{n+1} = -D_w^{n+1}/u_w^{n+1}, \qquad e_w^{n+1} = h_w^{n+1}/\gamma, \quad c_w^{n+1} = \sqrt{(\gamma-1) k h_w^{n+1}/\gamma} \tag{2.8}$$

If $u_w^{n+1} > c_w^{n+1}$, then $u_w^{n+1} = c_w^{n+1}$ and the iterations with respect to j are repeated. However, if $\varphi_w < \varepsilon_w$ or $q_0(t) = 0$, we assume that the vaporization wave has stopped and the new condition $u_w = 0$ has occurred. In this case the parameters of the vapor at the stationary boundary are taken as:

$$u_w^{n+1} = 0, \quad D_w^{n+1} = 0, \quad v_w^{n+1} = v_w{}^n + \Delta t u_w^{n+1} / (m_{w+1}^{n+1} - m_w^{n+1}) \tag{2.9}$$
$$E_w^{n+1} = E_w{}^n - \Delta t \left[\frac{u_w^{n+1} p_w{}^n}{m_{w+1}^{n+1} - m_w^{n+1}} + \left(\frac{\partial q}{\partial m} \right)_w^n \right]$$

where

$$\left(\frac{\partial q}{\partial m} \right)_w^n = q_0(t) \varkappa_w{}^n (1 + k_r) \varphi_w$$

Calculation of the iterations on the vaporization wave at the moment of vaporization renewal presents definite difficulties, since the velocity u_W increases sharply in a quite short time interval. Therefore at these moments the velocity u_W is initially taken from the nearest computational point. If u_W found from the conservation equations is still small in comparison with the speed of sound c_W, we assume that the vaporization wave has not yet renewed its motion. Stability analysis of the calcuation in the presence of a boundary, the vaporization wave, shows that the chosen computational scheme is always stable and there is no additional limitation on the time step Δt in comparison with the infinite problem.

Determining Velocity at the Vapor–Vacuum Boundary. To determine u_0^{n+1} the function u(m) is extrapolated to the vapor–vacuum boundary from the neighboring computational points completely analogously to the extrapolation of the velocity on the vaporization wave. Stability analysis of this boundary condition shows that the computational scheme chosen above is unconditionally stable.

Calculation of Radiation Flux. The total energy flux is found from the transport equations (1.4), written in integral form

$$F = F^+ + F^- = F_0(t) \exp\left(-\int_m^0 \varkappa dm \right) - k_r F_0(t) \exp\left(-\int_{m_w}^m \varkappa dm \right) \tag{2.10}$$

The value of $(\partial F/\partial m)$, and of $(\partial q/\partial m)$ in the planar case, is determined from the values of F or q at the edges of the given cell, i.e., at the points $\frac{1}{2}(m_i + m_{i-1})$ and $\frac{1}{2}(m_i + m_{i+1})$.

Calculation of Detonation Wave. As a result of detonation wave-front smearing, the temperature varies smoothly over several computational points. However, in the low-temperature region the absorption coefficient $\varkappa$ depends nonlinearly on the temperature – exponentially and with a large exponent.

The change of the radiation absorption coefficient from the values corresponding to the temperatures ahead of the shock wave front to the values corresponding to the temperatures behind the front is very large, several orders of magnitude. Therefore, not only is the absorption coefficient $\varkappa$ behind the detonation wave front so large that in this region the absorption must be accomplished by a mass smaller than the "computational interval" Δm, but also absorption becomes significant even within the shock wave front, in a zone whose width is determined by the artificial viscosity. As a result of this, the absorption effect begins essentially ahead of the detonation wave front, which leads to unstable propagation of this wave and irregular velocity of its motion.

To eliminate this phenomenon we adopted a special technique proposed by one of the authors, which can be termed "artificial broadening of the energy release zone." This technique was suggested by the real structure of the detonation wave.

The detonation wave is in essence a shock wave (i.e., a jump), whose actual width is determined by the actual viscosity and thermal conductivity. As a result of the abrupt temperature rise in this discontinuity (or in the narrow zone), there is a sharp increase of the radiation absorption coefficient (absorption initiation takes place) and intense absorption begins. Although the radiation mean free path may in itself be small, it is still considerably longer than the width of the viscous shock, and therefore the energy release zone is correspondingly wider (although it may be small in comparison with the characteristic dimensions of the problem).

When using the artificial viscosity the width of the viscous shock increases, although this width cannot be permitted to become larger than the energy release zone. Therefore it is necessary to artificially broaden the energy release zone also, at least enough so that it becomes somewhat larger than the viscous shock zone.

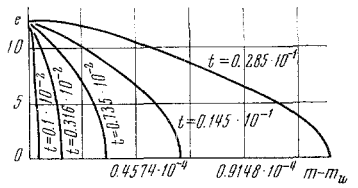

Fig. 1

To this end we used the technique of limiting the magnitude of the absorption coefficient $\varkappa$ on the basis of the condition $\varkappa \Delta m \leq \tau_m$, where τ_m is a constant which regulates the magnitude of the smearing (in the calculations presented τ_m, the maximal possible optical thickness of a single cell, was varied in the range 0.1-0.3). It is obvious that in this case the total width of the discontinuity becomes somewhat greater than in conventional shock waves. However, for a sufficiently large number of computational points this is not very significant, since it is still much less than the characteristic "dimension" of the entire problem, i.e., the total vaporized mass m_w^*, at the time t^* of occurrence of the flash. Therefore the energy-release zone propagation conditions correspond with sufficient precision to the conservation laws in the detonation wave.

The time step Δt is selected from stability considerations but is such that the vaporization wave's computational interval Δm will pass no faster than 10 time layers because of precision considerations. Since the vaporization wave is a moving boundary, the number of computational points with respect to mass is a variable quantity.

As soon as $m_{w+1} - m_w \geq \Delta m$, a mass point is added, at which all the quantities are interpolated between the vaporization wave point and the neighboring computational point. If the number of mass points reaches the maximal possible number (based on limited computer memory), then the scale is expanded (specifically, the number of mass points is halved. while retaining the internal and kinetic energy intervals.

3. COMPUTATIONAL EXAMPLE

In the present paper we consider as an example the plane case ($\nu = 1$). The objective is to demonstrate qualitatively the gasdynamic effects during the flash and subsequent heating. In place of the tabular equation of state we use the equation of state (1.5) of an ideal gas with $\gamma = k = \text{const} = 5/3$. We neglect condensation and absorption of the condensate. In place of the real vapor absorption coefficient, given in tabular form, we use an approximate analytic interpolational formula for the absorption coefficient, given in the form

$$\frac{1}{\varkappa} = \frac{1}{\varkappa_1} + \frac{1}{\varkappa_2}, \qquad \varkappa_1 = \varkappa_1^\circ \exp\left[b\left(1 - \frac{T_0}{T}\right)\right], \qquad \varkappa_2 = K\rho \tag{3.1}$$

Here $\varkappa_1^\circ$ is the value of $\varkappa$ for $T = T_0$. The function $\varkappa_1$ corresponds to absorption of weakly ionized vapors in the low-temperature region, when the change of the ionization degree α_e is described by the Boltzmann exponential relation. In the general case

$$b = \frac{d \ln \varkappa}{d \ln T} \text{ for } \quad T = T_0$$

If arresting absorption in electron–ion collisions is dominant, then $\varkappa \sim \alpha_e^2$ and $b = T/T_0$.

However, if arresting absorption in electron–neutral atom collisions is dominant, then $\varkappa \sim \alpha_e$ and $b = I/2T_0$.

The function $\varkappa_2$ describes approximately the vapor absorption in the region of those temperatures where single ionization is completed and multiple ionization proceeds. The values of the constants $\varkappa_1^\circ$, b, and K are taken from the tables of $\varkappa(e, \rho)$.

The initial values were selected on the basis of the known solution for adiabatic vapor flow in a centered expansion wave behind a vaporization wave travelling at constant velocity, with the Jouguet condition satisfied behind the vaporization wave front. From the given initial parameters m_w°, u_w°, p_w°, ρ_w°, corresponding to the selected initial time t_0 and flux $q_w = q_0$ (no screening), the initial distributions of the functions are found for $m_w^\circ \leq m \leq 0$

$$\frac{\rho_w}{\rho_w^\circ} = \left(\frac{m}{m_w^\circ}\right)^{2/(\gamma+1)}, \quad \frac{p}{p_w^\circ} = \left(\frac{\rho}{\rho_w^\circ}\right)^\gamma, \quad \frac{u}{u_w^\circ} = 1 + \frac{2}{\gamma - 1}\left[1 - \left(\frac{p}{p_w^\circ}\right)\right]^{(\gamma-1)/2\gamma} \tag{3.2}$$

As an example we considered the effect of radiation with constant flux density $q = 320$ mW/cm^2 on a carbon surface with exposure duration up to 2 μsec (this is a typical value of the duration of a single peak for free generation of radiation by a laser; exposure with shorter duration corresponds to the "giant pulse" regime).

Prior to initiation of screening, the vapor motion velocity u_w immediately behind the vaporization wave was 3.6 km/sec, the pressure p_0 on the surface ahead of the vaporization wave was 2700 kg/cm^2, the pressure p_w in the vapors behind the vaporization wave was 1000 kg/cm^2, the corresponding phase change temperature $T_w(p_w)$ was taken equal to 11900°K, and the vapor absorption coefficient $\varkappa_w$ at this temperature was assumed to be $7 \cdot 10^2$ cm^2/g.

This temperature is somewhat higher than that determined by extrapolating the experimental data. However, since we assumed $b = I/T_0$, the cited value of $\varkappa_w$ was taken without account for arresting absorption C during collision of electrons with neutral atoms, photodetachment of electrons from negative ions C^- and C_2^-, and molecular absorption C_2 and C_3, which reduces somewhat the value of $\varkappa$ for the same temperature. As a result, the value of $\varkappa_w$ does not differ markedly from $\varkappa_w$ from tables formulated with account for these effects.

The reflection coefficient k_r is taken as zero. The coefficient K for carbon is about $0.44 \cdot 10^8$ cm^5/g^2 for an incident radiation quantum energy of 1.78 eV, which corresponds to the radiation of a ruby laser.

Under these simplifying assumptions it is easy to obtain estimates of the characteristic parameters, which can be compared with the calculation itself. These estimates are presented below, after the description of the pattern of the process obtained as a result of the numerical calculation, which shortens their justification, since this is obvious from the computational results themselves (such estimates were actually obtained by one of the authors prior to initiating the calculations – during formulation of the problem). In making a quantitative comparison of the computational results for this example with experimental data, we must bear in mind that this comparison is to some degree merely illustrative, because of the simplifications made.

Figure 1 shows the distribution of the internal energy e(kJ/g) as a function of the mass $m - m_w$(g/cm^2) of vaporized matter at different moments of time t (μsec). It is easy to see that in the course of practically the entire time for which the distributions are shown, absorption is not significant and the distribution itself is close to the primitive distribution found from the self-similar solution of the problem of adiabatic vapor flow behind a vaporization wave travelling with constant velocity. Only on the last curve, corresponding to $t = 0.028$ μsec, do we note some increase of the internal energy above the values for the vaporization wave.

Figures 2 and 3 show respectively the distributions of the pressure p (kg/cm^2) and internal energy at the moment of development of the flash – the formation of a narrow hot layer, which is at the same time a high pressure layer.

Figures 4 and 5 show the same distributions in the stage of detonation wave formation and its propagation to the boundary with the vacuum. Comparison of Figs. 4 and 5 shows that the width of the energy release zone is actually somewhat greater than that of the pressure "jump" zone. In Fig. 4 we even see a zone of pressure decrease behind the shock wave front, which is associated with energy release in this region ("chem-peak"). The last curves in Figs. 4 and 5 correspond to the time ($t = 0.1$ μsec) when the detonation wave reaches the boundary with the vacuum. The energy release zone is now immediately adjacent to this boundary, and the maximal pressure, which previously corresponded to the shock wave front, now decreases sharply. Detonation wave crossing of the vapor–vacuum boundary is accompanied by marked acceleration of the "edge" particles. Increase of their velocity leads to more rapid expansion of the "peripheral" layers and reduction of their density, which facilitates penetration of the radiation into the deeper layers.

Figure 6 relates to the self-consistent heating and rarefaction wave propagation stage, ahead of which the shock wave front travels toward the surface of the solid body. In Fig. 6a we see that at about 0.22 μsec the shock wave reflects from the surface of the solid body, causing the pressure at the surface to increase sharply to values close to those which existed prior to onset of screening. By $t = 0.29$ μsec the reflected wave has already passed into the hot and low-density zone, as a result of which the pressure again begins to decrease. We see clearly in Fig. 6b that the hot region (where the energy of the incident radiation is released) gradually displaces toward the surface of the solid body. However, since the internal energy of the vapors in this zone exceeds considerably (by about one order of magnitude) the "effective combustion enthalpy" prior to initiation of screening, the rate of advance of the heating wave is approximately one order less than the rate of propagation of the vaporization wave prior to the flash.

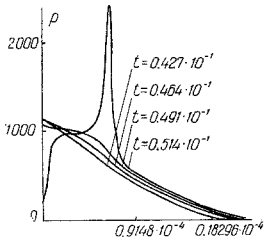

Fig. 2

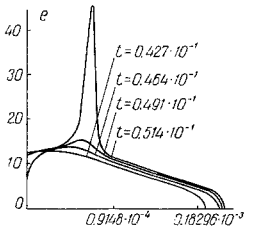

Fig. 3

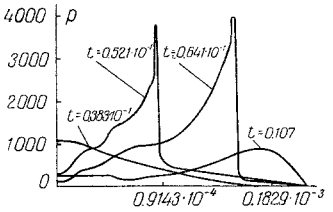

Fig. 4

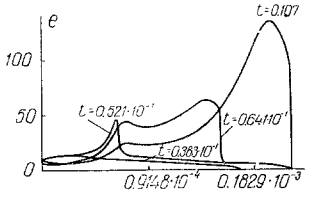

Fig. 5

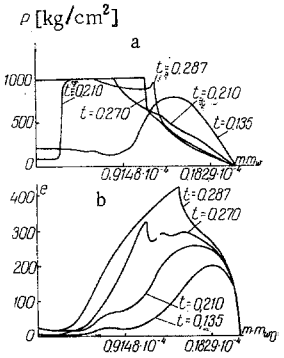

Fig. 6

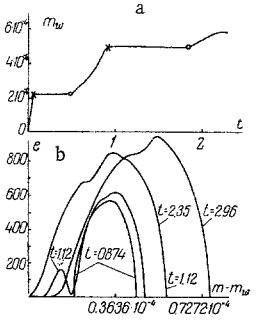

Fig. 7

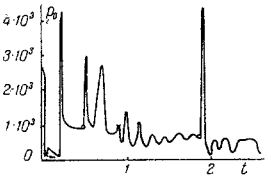

Fig. 8

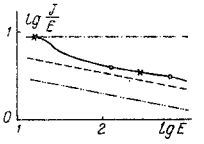

Fig. 9

Figure 7a shows the mass m_W (g/cm^2) of vaporized matter as a function of time t (μsec). After the dispersed mass (vaporized prior to initiation of the flash) of the layer again becomes transparent, vaporization renews. It is easy to see from Fig. 7a that this occurs approximately at the time 0.5 μsec. Now the hot vapors are essentially forced away from the vaporizing surface by the cold vapors entering "through" the vaporization wave at the equilibrium phase transition change temperature (we note that in Figs. 1-6 the parameter distributions are plotted as a function of the mass reckoned from the surface of the solid body). Then in this layer there is a new "flash" in the present case at a time of about 0.95 μsec. Its development and motion toward the vapor–vacuum boundary is clearly seen in Fig. 7b. Vaporization is renewed at a time of about 1.9 μsec.

In addition to the pressure oscillations at the surface of the solid body owing to the propagation of shock, compression, and rarefaction waves, there also appear sharp pressure changes caused by renewal of vaporization, seen in Fig. 8, where the pressure p_0 (kg/cm^2) at the surface of the solid body is shown as a function of time.

Figure 9 shows the logarithm of the ratio of the pressure impulse J (dyne · sec/cm^2) to the magnitude of the energy supplied E (J/cm^2) as a function of the logarithm of E. It is easy to see that this ratio decreases from the initiation of screening. This relationship is similar to that obtained experimentally [15], but for constant exposure duration, rather than for constant radiation flux, as in our calculations. It is curious that the impulse changes quite smoothly in spite of the strong pressure oscillations. In Figs. 7a, 8, and 9 the crosses denote the times of flash occurrence, and the circles are the times when vaporization renews. The relation which follows from the self-similar solution [9-11] is shown dashed. It is easy to see that the calculated relation is practically parallel to that obtained from the self-similar solution but lies somewhat higher. This is associated with the fact that in the numerical calculations we also took into account the adiabatic dispersion stage after switching off the source. Thus the curve of J/E versus E corresponds to a whole series of calculations for the same radiation flux but different exposure times. The dash-dot line shows J/E versus E without a flash.

Calculations have now been made using tables of the thermodynamic and optical properties of the matter and variable flux $q_0(t)$, which occurs in real pulses. These results for various substances and their analysis will be published separately.

4. ESTIMATES OF PRIMARY PARAMETERS

We shall now examine the estimates of the primary parameters (under the simplifying assumptions adopted above), which makes it possible to determine how these parameters change in comparison with the version discussed above with change of the incident radiation flux density and duration of the excitation process.

Flash Occurrence Criterion. Cooling owing to expansion becomes equal to the energy release owing to absorption. In the plane centered (with constant value of q_0) rarefaction wave following the vaporization wave, in which the relations (3.2) hold, this condition for points near the vaporization wave (temperature rise occurs in the hottest layers of the vapors) can be written in the form

$$\frac{1}{\rho_w}\left(\frac{\partial p}{\partial t}\right)_w = \frac{p_w}{\rho_w}\frac{dm_w}{dt}\frac{2\gamma}{m_w(\gamma+1)} = -\left(\frac{\partial q}{\partial m}\right)_w \tag{4.1}$$

Considering that at the moment t_* of vapor temperature rise initiation their layer is optically thin and consequently $q_W \approx q_0$, where q_0 is the radiation flux incident from outside, the term $(\partial q/\partial m_W)$ can be transformed to

$$(\partial q / \partial m)_w \approx \varkappa_w q_0 (1 + k_r)$$

Here we have considered that reflected radiation also causes heating of the vapors. Hence follows the criterion for initiation of screening

$$\frac{dm_w}{dt}\frac{p_w}{\rho_w}\frac{2\gamma}{(\gamma+1)} = m_w \varkappa_w q_0 (1 + k_r)$$

Here and hereafter we take q_0 and m_W^* to be their absolute values for convenience.

Since $(dm_W/dt) = m_W^*/t_*$, we have

$$t_* = \frac{p_w}{\rho_w}\frac{2\gamma}{(\gamma+1)}\frac{1}{\varkappa_w q_0 (1 + k_r)} \tag{4.2}$$

Using (1.11), we obtain

$$\frac{1-k_r}{1+k_r}\frac{(p_w/\rho_w)}{H}\frac{2\gamma}{\gamma+1} = \varkappa_w m_w^* \tag{4.3}$$

Since $(p_W/\rho_W) \ll H$, then $\varkappa_W m_W^* \ll 1$. For carbon $\varkappa_W m_W^* \approx 0.16$, for aluminum $\varkappa_W m_W^* \approx 0.015$ (for $k_r = 0.76$ [16]). The vapor's optical thickness $\tau < \varkappa_W m_W$ (because of the temperature decrease and corresponding reduction of $\varkappa$ in comparison with $\varkappa_W$ as the boundary with the vacuum is approached). Therefore, at the moment of flash occurrence $\tau_* \ll 1$, i.e., heating begins to take place with a practically completely transparent vapor layer (the condition (4.3) is local rather than integral). Calculations using (4.3) are in very good agreement with the results of the numerical calculations. As a result of the exponential variation of the phase equilibrium pressure with temperature in accordance with the Clapeyron–Clausius

formula and the exponential variation of the ionization degree and therefore of the absorption coefficient with temperature, we have $\varkappa_w = \varkappa_0 (p/p_0)^{\omega}$, where $\omega = d \ln \varkappa / d \ln p$ and in the present example $\omega = I_1/Q_a$, I_1 is the first ionization potential, and Q_a is the heat of vaporization per atom. For carbon $\omega \approx 2$. In accordance with (1.11) and (1.12), the pressure in the vaporization wave without screening is proportional to the incident radiation flux density q_0, specifically

$$p_w = q_0 (1 - k_r) / (Hc_w\gamma)$$

and the mass of the vapor layer at the moment t_* of occurrence of the flash is proportional to t_*; therefore from the criterion (4.3) follows $q_0^{\omega+1} t_* = \text{const}$ or $t_* \sim q_0^{-(\omega+1)}$. Thus, with increase of the radiation flux density q_0 for the same input energy $E = q_0\tau$ the screening initiation time t_* (and along with it the characteristic pressure pulsation time and the intervals between successive vaporization renewals) diminishes far more rapidly than the total exposure time τ, i.e., for large radiation flux densities the vaporization process can be considered continuous.

Pressure Decrease at Moment of Screening Initiation. After the flash the absorption coefficient in the heated region increases sharply, the magnitude of the radiation flux incident on the surface of the solid body decreases markedly, and vaporization terminates practically immediately. This is accompanied by reduction of the pressure at the surface of the solid body.

The pressure p_0 at the surface of the solid body decreases by $(\gamma + 1)$ times, i.e., about 2.7 times for $\gamma = 5/3$ (because of vaporization termination), to the pressure p_w in the vapors at the surface of the solid body behind the vaporization wave, and in addition, the pressure decrease continues because of the fact that prior to occurrence of the flash all the vapors had quite high velocity directed from the surface of the solid body. The change of the boundary condition at the surface from $u = c_w$ to $u = 0$ leads to the development of a rarefaction wave, since a pressure gradient is necessary to stop the gas travelling along the surface. We shall assume that vaporization terminates abruptly (this is not too bad an idealization because of the extremely abrupt nature of the vapor layer's optical thickness growth and the corresponding reduction of the radiation flux to the surface of the solid body).

For times which do not differ too much from the moment of the flash, the resulting rarefaction wave can be considered to be centered; consequently, we have the equations

$$m - m_w^* = \rho_w c_w (t - t_*), \quad u - 2(c - c_w)/(\gamma - 1) = c_w \tag{4.4}$$

The constant c_w in the Riemann invariant is found from the condition that the rarefaction wave propagates through the gas, where $c = c_w$, $u = c_w$, at least at those moments of time when the wave boundary has not yet moved markedly away from the surface of the solid body. At the surface of the solid body, where the condition $u = 0$ is now satisfied, we obtain from (4.4)

$$\frac{c}{c_w} = \frac{3 - \gamma}{2} \tag{4.5}$$

Correspondingly, the pressure p_0 at the surface changes as follows

$$\frac{p_0}{p_w} = \left(\frac{c}{c_w}\right)^{2\gamma/(\gamma-1)} = \left(\frac{3-\gamma}{2}\right)^{2\gamma/(\gamma-1)} \tag{4.6}$$

For $\gamma = 5/3$ we obtain a pressure decrease by about a factor of 20. We note that this quantity depends quite strongly on the adiabatic exponent γ, and for $(\gamma - 1) \ll 1$, which holds with account for vapor condensation, when the vapor flow is nearly isothermal, the pressure drop is not so large.

Development of Heating-up Process. We shall assume that heating-up after the time t_* takes place at constant density (the temperature rise rate with account for expansion of the medium at constant pressure, for example, will differ very slightly from that found, since the heat capacities C_p and C_v are similar). The equation describing the temperature variation has the form

$$\frac{\partial e}{\partial t} = \varkappa q_0 (1 + k_r) \tag{4.7}$$

For simplicity we set $C_v = \text{const}$, and we approximate $\varkappa(T, \rho)$ by the exponential relation (3.1) for $T_0 = T_w$ and $K = 0$. For $b/T_w \ll 1$ a comparatively small temperature increase leads to a significant increase of the absorption coefficient. The temperature rise rate increases correspondingly. Consequently, most

of the warm-up time (after initiation of warm-up) is spent at comparatively low temperatures. Expanding T_w/T into a series in $\theta = \Delta T/T_w$ and considering only the first term, we obtain

$$\frac{\partial \theta}{\partial t} = \exp(b\theta)\frac{\varkappa_w q_0 (1+k_r)}{C_v T_w} \tag{4.8}$$

The solution of this equation has the form

$$1 - \exp(-b\theta) = \frac{\varkappa_w q_0 (1+k_r)]}{C_v T_w} b(t - t_*) \tag{4.9}$$

We see that, regardless of the degree of heating $\theta_k(t_k)$ taken to be significant, for $b\theta_k \gg 1$ we obtain

$$t_k - t_* = p_w / [\rho_w b \varkappa_w q_0 (1 + k_r)(\gamma - 1)] \tag{4.10}$$

Considering (4.2), we obtain

$$t_k - t_* = (\gamma + 1)t_* / [2\gamma(\gamma - 1)b] \tag{4.11}$$

Thus, for $b \gg 1$ the heating time $t_k - t_*$ is comparable with the time t_* of temperature rise initiation or even considerably shorter. We note that when the vapors do not expand into a vacuum (significant resistance of the air or of the vapors themselves during subsequent flashes), the absence of a pressure differential in the vapor region eliminates the critical nature of the heating process; it will exist practically from the very beginning and the heat-up time can be estimated from (4.10) for $t_* = 0$. We see from (4.11) that absence of a pressure differential leads to considerable shortening of the heating time.

Amplitude of the Shock Wave Propagating from the Heating Zone. Let us estimate the magnitude of the pressure p_f in the heating zone, assuming that it is constant within the entire layer being heated and outside the layer up to and including the shock wave but, naturally, is not equal to the pressure p_w in the vapor layer prior to initiation of heating. Then we obtain from the energy equation (1.3)

$$\frac{\partial h}{\partial t} + \frac{\partial q}{\partial m} = 0 \tag{4.12}$$

Setting $\gamma = \text{const}$ and $p_f = \text{const}$, we obtain

$$\frac{\partial h}{\partial t} = \frac{p_f \gamma}{(\gamma - 1)}\frac{\partial v}{\partial t}, \qquad \frac{\partial v}{\partial t} = -\frac{(\gamma - 1)}{p_f \gamma}\frac{\partial q}{\partial m} \tag{4.13}$$

Using (4.13), the continuity equation (1.2) can be rewritten in the form

$$\frac{p_f \gamma}{(\gamma - 1)}\frac{\partial u}{\partial m} + \frac{\partial q}{\partial m} = 0 \tag{4.14}$$

Integrating (4.14), we obtain

$$[p_f \gamma / (\gamma - 1)]\ u = -q + \text{const} \tag{4.15}$$

Two shock waves with the same amplitudes propagate in both directions from the heating region. Hence the shock wave velocity u_f can be found from the relation

$$2\gamma p_f \Delta u_f = (\gamma - 1)|q_0|, \quad u_f = \pm \Delta u_f + u_w \tag{4.16}$$

We note that the shock wave travelling toward the surface of the solid body is weakened as it interacts with the rarefaction wave described above. Let us assume that the shock wave will be a wave of moderate intensity (travelling opposite the radiation), i.e., we use the following expansion of the shock adiabat [12]:

$$p_f - p_w = \Delta p = m^* \Delta u_f, \quad m^* = \rho_w c_w [1 + {}^1/_4 (\gamma + 1)\eta] \tag{4.17}$$

Here η denotes $\Delta u_f / c_w$.

Equation (4.17) is easily transformed to

$$p_f / p_w = 1 + \gamma [1 + {}^1/_4 (\gamma + 1)\eta]\eta \tag{4.18}$$

Using the relations across the vaporization wave, we obtain from (4.16)

$$2(1 - k_r)\eta(p_f / p_w) = H / h_w \tag{4.19}$$

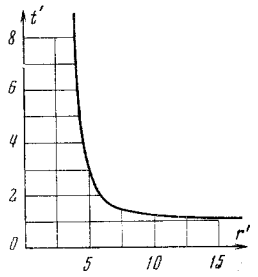

Fig. 10

From (4.18) and (4.19) we obtain the following equation for finding η:

$$H / h_w = 2(1 - k_r)\eta \{1 + \gamma [1 + {}^1/_4 (\gamma + 1)\eta]\eta\} \quad (4.20)$$

Solving this equation for $H/h_W = 3$, $\gamma = {}^5/_3$, $k_r = 0$, we find that

$$\eta = 0.60,\ \Delta T / T_w = (T_f - T_w) / T_w = 0.42,\ \Delta p / p_w = (p_f - p_w) / p_w = 0.84,\ \Delta c / c_w = (c_f - c_w) / c_w = 0.20.$$

We note that these parameters justify use of the moderate amplitude wave approximation. It is not essential in practice whether or not the increase of the pressure and heating occurs in a shock wave or in a compression wave. A temperature increase by a factor of 1.4 is sufficient for very marked increase of the absorption coefficient – by 20 times for $b = I/T_W \approx 10$. We note that this estimate of the shock wave amplitude shows that the structure of the heating zone is quite unimportant, which naturally avoids the need for using any special methods for the numerical calculation of this narrow zone.

Parameters of Detonation Wave from Heating Zone. The relations across the strong detonation wave front, which is maintained by an incident radiation front, were presented in [7, 8]. However, in the present case the backpressure is significant and the relations have the form:

continuity equation

$$m_d' (v_d - v_1) = -\Delta u = -(u_d - u_1) \quad (4.21)$$

equation of motion

$$m_d' \Delta u = p_d - p_1 \quad (4.22)$$

energy equation

$$m_d' [e_d - e_1 + {}^1/_2 (u_d^2 - u_1^2)] + p_d u_d - p_1 u_1 = -q_0 \quad (4.23)$$

Jouguet condition

$$m_d' = \rho_d c_d \quad (4.24)$$

equation of state

$$e_d = p_d v_d / (\gamma_d - 1),\ e_1 = p_1 v_1 / (\gamma_1 - 1) \quad (4.25)$$

Here the subscript d relates to the state behind the detonation wave front, and the subscript 1 applies to the states ahead of the front, and $m_d > 0$ for $q'(t) < 0$, since the wave travels opposite the radiation flux. Considering that the speed of sound equals $c_d = \sqrt{k_d p_d v_d}$, we obtain from (4.21)-(4.25):

detonation velocity

$$m_d' = \rho_1 c_d [1 + (1 / k_d)\ (1 - p_1 / p_d)] \quad (4.26)$$

internal energy behind detonation wave front

$$e_d = e_1 \frac{(p_d / p_1)[(\gamma_1 - 1)/(\gamma_d - 1)]}{1 + [(1 + p_1/p_d)/k_d]} \quad (4.27)$$

specific volume behind detonation wave front

$$v_d = v_1 / \{1 + [(1 + p_1 / p_d) / k_d]\} \quad (4.28)$$

Since in this case the detonation wave travels through gas with parameters close to those behind the vaporization wave prior to initiation of screening ($p_1 \approx p_W$, $\rho_1 \approx \rho_W$, $h_1 \approx h_W$), neglecting the differences between γ_d and γ_i and between k_d and γ_d and taking into account the relations across the vaporization wave, for large values of the pressure ratio $y = p_d/p_1$ across the detonation wave we can obtain the following expression for finding y:

$$\frac{H}{h_w} = (1 - k_r)\sqrt{yY}\left\{\frac{y}{Y}\left[1 - \left(1 - \frac{1}{y}\right)\frac{\gamma - 1}{\gamma}\left(1 + \frac{1}{2\gamma}\left(1 - \frac{1}{y}\right)\right)\right] - 1\right\},\quad Y(\gamma, y) = 1 + \frac{1}{\gamma}\left(1 - \frac{1}{y}\right) \quad (4.29)$$

For the typical value $H/h_W = 3$ and $k_r = 0$ we find that $y \approx 5.2$; then according to (4.28) the density ratio $\rho_d/\rho_W = 1.48$ and, consequently, the ratio p_d/ρ_d increases by 3.6 times in comparison with p_W/ρ_W. In ac-

cordance with (4.26), the detonation wave propagation velocity equals $2.8\,|\,m_w^{\cdot}\,|$, i.e., the detonation wave travels opposite the radiation flux with considerably greater velocity than the vaporization wave travels in the positive direction of the vaporization wave under the action of the same radiation flux q_0. It is curious that the detonation wave's relative amplitude is practically independent of the incident radiation flux density.

Self-Consistent Rarefaction and Heating Wave. If the temperature of the substances in the region where the radiation energy is released is considerably higher than that of the vapors ahead of the heating wave, and the characteristic vapor density in the wave exceeds considerably the vapor density ahead of the wave, then the solution can be obtained by using the solution of the self-similar problem [9-11] for the absorption coefficient dependence, given in the form $\varkappa = K\rho$ (we note that self-similar solution is valid, strictly speaking, only for infinite vapor density ahead of the wave and for absolutely cold gas ahead of the wave). The dependences of the maximal pressure p_m, maximal internal energy e_m, and heated mass m on the time t and radiation flux density q_0 will have the form

$$p_m = P_m (Kt)^{-1/5} q_0^{\,3/5}, \quad e_m = E_m (Kt)^{2/5} q_0^{\,4/5}, \quad m = \mu_m (Kt)^{-2/5} q_0^{\,1/5} t \tag{4.30}$$

The values of P_m, E_m, μ_m are given by the following table, obtained by V. M. Krol' by a technique similar to that he used in [11] for other power-law relations $\varkappa(e, \rho)$

$\gamma =$	5/3	7/5	6/5
$P_m =$	0.747	0.627	0.468
$E_m =$	0.517	0.712	1.015
$\mu_m =$	1.260	1.170	1.050

Effect of Two-Dimensionality on Screening Development Time. We have examined only the planar case. However, in view of the limited size of the irradiated spot, lateral spreading of the vapor jet may begin if the exposure process continues long enough. In order to evaluate the effect of lateral spreading on the time for initiation of the flash, we calculated a similar problem, but for radially symmetry vapor flow from a vaporizing sphere.

Figure 10 shows the ratio t' of the time t_3^* for initiation of the flash in the spherical case to the time t_1^* for initiation of the flash in the planar case as a function of $r' = r_0/c_w t_1^*$, where r_0 is the radius of curvature of the irradiated surface. We see that lateral spreading "suppresses" the onset of screening. This is associated with the fact that for $t \geqslant (r_0/c_w)$ a quasistationary regime is established, in which the pressure gradients near the vaporizing surface no longer change; while in the planar case these gradients decrease continuously as the layer thickness increases. However, in the case in which screening begins in the planar spreading stage, lateral spreading leads to establishment of the quasistationary vapor motion and heating regime [6].

In this case, according to [6], the following parameter variation relations will hold (for the case $\varkappa = K\rho$):

$$e \sim q_0^{2/3} (Kr_0)^{1/3}, \quad p \sim q_0^{2/3} (Kr_0)^{-1/6}, \quad u \sim q_0^{2/3} (Kr_0)^{1/6}, \quad \rho \sim (Kr_0)^{1/2}$$

We wish to thank P. V. Kevlishvili for assistance in carrying out the present study.

LITERATURE CITED

1. J. F. Ready, "Effects due to absorption of laser radiation," J. Appl. Phys., vol. 36, no. 2, 1965.
2. S. I. Anisimov, A. M. Bonch-Burevich, M. A. El'yashevich, L. A. Imas, N. A. Pavlenko, and G. S. Romanov, "Effect of powerful light fluxes on metals," Zh. tekh. fiz., vol. 36, no. 7, 1966.
3. Yu. V. Afanas'ev and O. N. Krokhin, "Vaporization of matter under the action of laser radiation," ZhETF, vol. 52, no. 4, 1967.
4. V. K. Pustovalov and G. S. Romanov, "Scattering of matter from intensely vaporizing metal surface," Vestsi AN BSSR, Ser. fiz.-mat. navuk, no. 4, 1967.
5. I. F. Zharikov, I. V. Nemchinov, and M. A. Tsikulin, "Investigation of the influence exerted on a solid by luminous radiation from a source of the explosive type," PMTF [Journal of Applied Mechanics and Technical Physics], vol. 18, no. 1, 1967.
6. I. V. Nemchinov, "Stationary motion regime of vapors heated by radiation in presence of lateral spreading," PMM, vol. 31, no. 2, 1967.
7. Ya. B. Zel'dovich and Yu. P. Raizer, Physics of Shock Waves and High-Temperature Hydrodynamic Phenomena [in Russian], Nauka, Moscow, 1966.

8. Yu. P. Raizer, "Breakdown and heating of gases under action of laser beam," Usp. fiz. n., vol. 87, no. 1, 1965.
9. O. N. Krokhin, "Self-consistent regime of plasma heating by laser radiation," Zh. tekhn. fiz., vol. 34, no. 7, 1964.
10. Yu. V. Afanas'ev, V. M. Krol', O. N. Krokhin, and I. V. Nemchinov, "Gasdynamic processes in laser heating of matter," PMM, vol. 30, no. 6, 1966.
11. V. M. Krol', "Planar self-similar motion of heat-conducting gas heated by radiation," PMTF, vol. 9, no. 4, 1968.
12. R. Courant and K. O. Friedrichs, Supersonic Flow and Shock Waves [Russian translation], Izd-vo inostr. lit., Moscow, 1950.
13. K. S. Shifrin, Light Scattering in Turbid Medium [in Russian], Gostekhizdat, Moscow-Leningrad, 1951.
14. R. D. Richtmyer, Difference Methods for Initial-Value Problems [Russian translation], Izd-vo inostr. lit., Moscow, 1960.
15. D. W. Gregg and S. J. Thomas, "Momentum transfer produced by focussed laser giant pulses," J. Appl. Phys., vol. 37, no. 7, 1966.
16. N. G. Basov, V. A. Voiko, O. N. Krokhin, O. G. Semenov, and G. V. Sklizkov, "Reduction of reflection coefficient of strong laser radiation from the surface of a solid substance," Zh. tekhn. fiz., vol. 38, no. 11, 1968.